Journal of Applied Mathematics and Physics, 2025, 13(7), 2418-2440
https://www.scirp.org/journal/jamp
ISSN Online: 2327-4379
ISSN Print: 2327-4352

Solution Due to Sinc Methods of Numerical Analysis: Three Type Sterile Neutrinos and the Longitudinal Massless with Flavor Changing of Missing Transverse Masses

Hung-Te Henry Su[1*], Po-Han Lee[2#]

[1]Department of Physics, Chung Cheng University, Chia-Yi, Taiwan Region
[2]Department of Electro-Optical Engineering, Taipei University of Technology, Taipei City, Taiwan Region
Email: hydrogen0221@gmail.com, leepohan@gmail.com

How to cite this paper: Su, H.-T.H. and Lee, P.-H. (2025) Solution Due to Sinc Methods of Numerical Analysis: Three Type Sterile Neutrinos and the Longitudinal Massless with Flavor Changing of Missing Transverse Masses. *Journal of Applied Mathematics and Physics*, **13**, 2418-2440.
https://doi.org/10.4236/jamp.2025.137138

Received: January 15, 2025
Accepted: July 26, 2025
Published: July 29, 2025

Abstract

The Daya Bay Collaboration has discovered that approximately 6.0% of active neutrinos were missing from the nuclear reaction container. This finding has led to a reinterpretation of the three known types of neutrinos. In this paper, we present an analysis based on deductive reasoning, proposing that neutrinos are massless in the longitudinal direction (referred to as "longitudinal massless"). This insight contributes to the broader body of literature on the subject. Additionally, our work resolves the long-standing mystery of CP conservation in strong interactions. Using advanced physical mathematics, we derive a significant result: the transformation between the third type of neutrino and photons or gravitons. We express the probability of this transformation in quantum mechanics using sinc functions which arise from interference effects, providing analytical solutions. Furthermore, considering the mass constraints imposed by the seesaw mechanism—referred to here as the "compete mechanism" (a generalized seesaw model)—we argue that the actual phase $\pi/4$ of CP violation precisely answers the fundamental question at hand.

Keywords

Daya Bay Collaboration, Neutrino Types, Longitudinal Massless, CP Conservation, Strong Interactions, CP Violation

1. Introduction

Active neutrinos were identified within the Standard Model through the mechanism

*First author.
#Corresponding author.

of neutrino oscillations. The nature of sterile neutrinos, however, remains a subject of theoretical investigation. Some sterile neutrinos are hypothesized to have sufficiently large masses and are referred to as "heavy neutral leptons" (HNLs or NHLs) [1]. Additionally, while active neutrinos possess left-handed masses, sterile neutrinos are associated with right-handed masses, implying the absence of left-handed masses in sterile neutrinos. In 1954, C.N. Yang and Robert Mills extended quantum electrodynamics (QED) by developing Yang-Mills theory, which generalized gauge theory from commutative (Abelian) groups to non-commutative (non-Abelian) groups in an effort to explain strong interactions [2]. However, their theory faced criticism from Wolfgang Pauli, who argued that in order to maintain gauge invariance, the quantum particles in Yang-Mills theory must be massless. Since such massless particles had not been observed in nature, the theory was initially set aside. It was not until the 1960s that the significance of Yang-Mills theory was recognized. Physicists Yoichiro Nambu, Geoffrey Goldstone, and Giovanni Jona-Lasinio introduced the concept of spontaneous symmetry breaking, which provided a framework for understanding how particles could acquire mass within Yang-Mills theory. This development ultimately led to the incorporation of massive particles into the theory. Although the existing framework has been effective in interpreting the mechanism by which particles acquire mass, this paper provides a well-developed solution to the challenges associated with *masslessness*. Our findings present strong evidence supporting *masslessness*, particularly through the observation that missing transverse mass exceeds longitudinal mass. In this study, we reveal the concept of *longitudinal masslessness* and identify three types of neutrinos, with the third type analyzed using advanced physical mathematics and deductive reasoning. Building on this foundation, we derive a key result related to the *top-point* of a triangle, where the "transforming point", $r_{Yuka} \approx 1.940$ fm, corresponds to photons and a fixed CP-violation phase angle $\delta_{CP} = \pi/4 < \pi/3$. This result leads to CP invariance, providing a resolution to the long-standing "strong CP problem". Based on this deduction, we propose that certain gauge bosons—such as massless photons or gravitons—may undergo transformations into one another as they travel through the universe. However, this phenomenon remains an open mystery. In this paper, we refine the interpretation of neutrinos as possessing three distinct types and provide a deductive analysis of their longitudinal *masslessness*. This work contributes to the broader literature and offers a potential resolution to the issue of CP conservation in strong interactions. Additionally, our approach addresses the previously insufficient explanation—namely, the assumption that the disappearance of 6.0% of sterile neutrinos could be justified without clear underlying reasons [3]-[5]. The concept of sterile neutrinos has been widely discussed in the literatures [6]-[25]. One of the recommended solutions to this problem is presented in this paper.

2. Method

2.1. Fundamental Concepts by Daya Bay Collaboration Data

We primarily examine recent neutrino oscillation probability data from the Daya

Bay Collaboration. i.e.,[1]

$$\sin^2\left(2\theta_{13}\right) \tag{1}$$

Moreover, let Eq. (1) be squared root as[2]

$$\psi \equiv \sin\left(2\theta_{13}\right) \tag{2}$$

Based on the data results, we use the cited data as a method to construct our analysis.

$$s_{13} + c_{13} = Const \tag{3}$$

Linearly in U_{CKM} (where $s_{13} \equiv \sin\left(2\theta_{13}\right)$, and $c_{13} \equiv \cos\left(2\theta_{13}\right)$). Therefore,

$$\begin{aligned} &\sin\psi + \cos\psi = Const, \\ &\sin\left(\sin\left(2\theta_{13}\right)\right) + \cos\left(\sin\left(2\theta_{13}\right)\right) \end{aligned} \tag{4}$$

This is approximately according with the form shown as

$$1 + \frac{\sinh\left(\delta\right)\big|_{\delta=1/2}}{2} \tag{5}$$

As derived in a previous paper, the corresponding of that study indicates that the three types of sterile neutrinos are positioned along the three sides of an equilateral triangle. Based on the mass acquisition mechanism illustrated in **Figure 2** with **Figure S3** by this paper, neutrino masses arise precisely from the addition of sterile neutrinos. This confirms that incorporating sterile neutrinos into current theories is both accurate and theoretically justified. Consequently, our interference framework remains self-consistent. Notably, ψ^2 in Eq. (2), the parameter could represent a scalar field (e.g., $g_{\alpha\beta}$ or Higgs fields or other relevant scalar fields). Given the properties of an equilateral triangle, there must be three distinct types. Furthermore, Eq. (4) also necessitates three types, as evident from the phenomenon of *chiral symmetry breaking*. We will examine this in details in section B of the results.

2.2. Interpretation for Neutrino Masses (An Examination of Self-Consistency)

Fundamental hypothesis: Suppose that the four-dimensional universe represents the external surroundings of infinite potential wells in the context of sterile neutrinos, based on brane theory. In this framework, the wave functions of sterile neutrinos in quantum mechanics satisfy the linear equations, such as Eq. (3) and Eq. (4) in this paper, where $\pi/4$ is precisely the initial phase angle for CP violation. This formulation suggests that sterile neutrinos exhibit tunneling behavior into the lower-dimensional (4-D) universe, consistent with the concept of D-branes. Such tunneling occurs from an infinite potential well, where a specific condition on $E_n = \infty$ is required (see **Figure 1**). If the opportunity arises, experimental observations may be able to detect this phenomenon. Remarkably, our

[1]Data shown as $\sin^2\left(2\theta_{13}\right) \approx 0.084 \pm 0.005$.

[2]Data shown as $\psi \equiv \sin\left(2\theta_{13}\right) \approx 0.2983, 0.2811$.

findings indicate that the rest mass of these neutrinos is zero (*longitudinal masslessness*). Additionally, we have derived an approximate solution to the linear equation. In the following sections, we present a step-by-step analysis.

Step I: The solution for the eigenfunctions of an infinite potential well is derived based on the framework presented in S. Reich's work (2012):

$$\Psi_n = \sqrt{\frac{2}{a}}\sin\left(\frac{n\pi x}{a}+\delta_{CP}\right)\Big|_{\substack{a=1,x=\frac{a}{3}\\ n\pi x=\frac{\pi}{3},\delta_{CP}=\frac{\pi}{4}}} \tag{6}$$

The following expression is nearly identical to Eq. (6):

$$\begin{aligned}\Psi_n &\approx \sin\left[\sin\left(\frac{\pi}{3}\right)\right]+\cos\left[\sin\left(\frac{\pi}{3}\right)\right],\\ \Psi_n &= \sin\left[\sin\left(\frac{\pi}{3}\right)\right]+\cos\left[\sin\left(\frac{\pi}{3}\right)\right]+C\end{aligned} \tag{7}$$

Here, $C \equiv 0.3510$ is precisely tuned to match the eigen-solutions of infinite potential wells in quantum mechanics, resulting in exact solutions. Specifically, the second formula in Eq. (7) is equivalent to Eq. (6). This step is constructed as described in Section 2.1.1.

Step II: The longitudinal mass $\left(m_y\right)$ of sterile neutrinos is zero due to the eigenvalues:

$$E_n \equiv \frac{n^2\pi^2\hbar^2}{2mL^2} = \infty, n \neq \infty, L \neq 0 \tag{8}$$

This requires $m = 0$ for tunneling from the infinite potential well, a result that also aligns with the zero-area condition of an isosceles trapezoid. However, it remains uncertain whether the speed of sterile neutrinos approaches the speed of light *C*. Since this discussion focuses on longitudinal mass, it is important to note that transverse mass $\left(m_T\right)$ is absent in the left-chiral system.

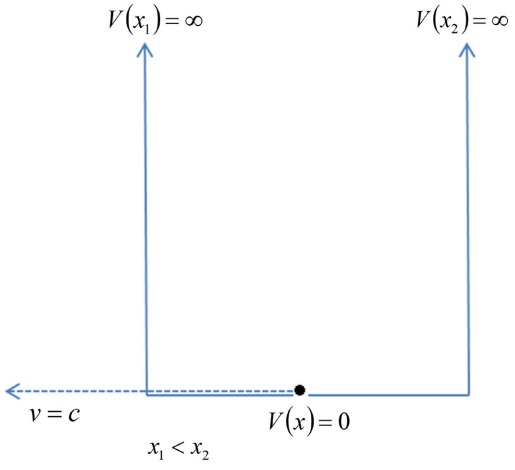

Figure 1. The sterile neutrino tunnels through the left-hand side of the infinite potential wall at the speed of light, *C*, without any scattering angle during tunneling. The wave-

particle duality of neutrinos would be illustrated in Figure 2.

The total speed of this quantum system (i.e., the wave packet) and whether it reaches C remains unknown and must be determined through experimental measurements. Nevertheless, based on its longitudinal *masslessness*, we propose that sterile neutrinos function as quasi-gauge fermions[3]. Through theoretical analysis in Section 2.4, we will further demonstrate that they may still undergo flavor-changing interactions in quantum mechanics (see Table 1).

3. Results and Discussion

3.1. Information and Profiles of Sterile Neutrinos (SN)

Table 1. Profiles of sterile neutrinos.

Masses	Nature of Particles	Suppose Primary
$m = 0$ (massless).		
1) It is accompanied by a scalar field with an extremely small mass, approximately zero ($< 2.30 \times 10^{-50}\ \text{kg} \to 0$)[a] but still greater than zero. However, in practice, this mass is effectively negligible. 2) Since transverse masses are absent in the left-chiral system, flavor-changing processes may occur. 3) Missing transverse masses can be determined using the wavelengths of matter waves described by Bessel functions, according to de Broglie relations (see later). This approach further allows for obtaining the reverse solution for m.	1) This paper proposes the nature of gauge fermions, which can be observed on the left-hand side (LHS). 2) ≤50%[b] represents the transformation probability for the third type of sterile neutrinos. 3) Classification of sterile neutrino types[c] **1st Type**: Left-chiral sterile neutrino (SN) **2nd Type**: Right-chiral sterile neutrino (SN) **3rd Type**: A_1 -SN (included in the right-chiral system)	1) Masses are related to helicity $(\sim \hbar/2)$, which needs to be verified as a potential aspect of a candidate for a theory of everything. 2) The helicity described above remains open to debate.

[a]There are strong reasons to believe that the third type of sterile neutrinos can inter-transform with photons $\left(< 1.78 \times 10^{-54}\ \text{kg}\right)$ or gravitons in quantum field theory (QFT). This will be thoroughly addressed in Appendix C. [b]Theoretical calculations for this probability can be found in Appendix D. Notably, the result aligns with the observed disappearance of approximately 6.0% of active neutrinos. Specifically, when excluding the third type of sterile neutrinos and disregarding the missing left-handed sterile neutrinos, only the second type of sterile neutrinos remains. If this remaining fraction of 0.25 is squared, it, $\left(\frac{1-50\%}{2}\right)^2 = 6.25\%$, yields an approximate 6.0% probability for the disappearance of active neutrinos. [c]They will be associated with the abbreviation LARSN, pronounced "Larsen". **Note:** About above, see Figure S2 (the seesaw mechanism).

3.2. Examinations for Chiral Symmetry Breakings

Applying the method we previously introduced, Eq. (4) transforms into Eq. (9),

$$\sin\left(\sin\left(2\theta_{13}\right)\right) + \cos\left(\sin\left(2\theta_{13}\right)\right) \approx 1.2497, 1.2382 \tag{9}$$

Aligning with the calculation of Eq. (5), which now becomes

$$1 + \frac{\sinh\left(\delta\right)\big|_{\delta=1/2}}{2} \approx 1.2605 \tag{10}$$

Examine the chiral symmetry in light of the closer solution of Eq. (9), which 1.2497 is better chosen than 1.2382 (since that $1.2605 > 1.2497 > 1.2382$), i.e., by

constructing

$$\varphi_R \equiv \frac{1+\varepsilon^5}{2} \approx 1.2497 \tag{11}$$

Thus, we obtain

$$\varepsilon \approx 1.0844 \tag{12}$$

Both Eqs. (11) and (12) satisfy the nature of right-handed Dirac spinors. Substituting Eq. (12) into $\varphi_L \equiv \frac{1-\varepsilon^5}{2} \approx -0.2498 < 0$, we find that it is of first-order smaller than the former, revealing that chiral symmetry breaking has occurred at 10^{-6} sec (precisely, this represents a chiral phase transition, though the exact phase remains unknown at present). However, based on the properties of an isosceles trapezoid, only one type must remain, leading to the right-handed neutrino $\varphi_R \approx 1.2497$ being the chosen state. This implies that left-handed neutrinos are excluded, or alternatively, they may be considered missing. In this paper, we have presented the above findings to physicists and astronomers to explain the mechanism behind the asymmetry between matter and antimatter in the current universe. However, there remains a probability of detecting left-handed neutrinos, as suggested by Eqs. (1) - (4). This examination is crucial, as it provides a correct determination of the chiral symmetry of sterile neutrinos.

3.3. The Recommended Solution for Strong CP Problem

For the previous third footnote:

See **Figure S3**, where the source may originate from the triangle without containing the point of A_1. In Eq. (6) (see Ref. [1]), $x = a/3$ with an angle of $\pi/3$, it reveals that the magic momentum of $\gamma = 29.30$ for electric field correction—under certain contexts—is precisely defined without considering electromagnetic (EM) fields. In this case, only the effects of strong interactions remain.

Notably, this occurs at $r_{Yuka} \approx 1.940$ fm, corresponding to the top point (where photons are located at the total symmetrical center of flavors) and must be associated with an angle. Thus, Eq. (6) corresponds to its quantum mechanical (QM) wavefunction solution, which forms an equilateral triangle in **Figure S3**. The boundary appearing along the x-axis is indicated as $x = a/3 = B$, where a represents the total length of the equilateral triangle, giving $\pi/3$ to each angle (here, we set $a \equiv 1$ for convenience).

This result is remarkable: although $\delta_{CP} = \pi/4 < \pi/3$ universally acts on all particles (e.g., neutrinos), CP conservation in strong interactions still holds. This is due to the equilateral triangle structure and $\delta_{CP} = \pi/4 < \pi/3$, which in this case leads to "CP invariance". This paper resolves a longstanding mystery that has not been addressed in previous studies. Furthermore, based on this, we could also set $\bar{\theta} \equiv 0$, which would yield the same results as found in the literatures. Moreover, this advanced setup aligns with the widely known "two-time dimensions" theory (i.e., $p^2 = 0$, massless in Eq. (11) according to the theory), first proposed in 1998

by Bars, Deliduman, and Andreev. This approach does not require a radical reworking of axion theory.

Our next goal is to investigate whether the axion (10^{-2} eV/c^2) [19], [20] is or is not the missing transverse mass of a sterile neutrino. Specifically, we aim to verify whether the transverse mass of the sterile neutrino serves as the source of the pseudoscalar field. The details of this investigation will be published in a forthcoming paper.

Additionally, we have recently identified the mathematical form of its wave packet, which is expressed in terms of Bessel functions. Notably, our findings 1/3 reveal that there are three types of sterile neutrinos, as their masses are constrained within a triangular region. If the axion is not the missing transverse mass of a sterile neutrino, this would lead to consistency between our findings and the "two-time dimensions" theory proposed by Bars, Deliduman, and Andreev.

3.4. Sources of Masses

The source of the masses could be attributed to CKM absorption of $g_{\alpha\beta}$. This process represents a second-order nonlinear optical absorption mechanism. The matrix absorption refers to the incorporation of the metric tensor from General Relativity into the intrinsic neutrino theory, where it induces non-human parameter adjustments within the CKM matrix.

3.5. Flavor Changing Remains in QCD

The invariance of flavor changing is considered in this case $|v_T| < c$. As shown in **Figure 2**, time flows with $t' = \gamma t_0$, and flavor changing of sterile neutrinos occurs within the framework of QCD.

3.6. Representation of Momentum Conservation

Momentum conservation in field-theory: The velocity of sterile neutrinos is determined using the momentum conservation expression and is defined as:

$$\cos\bar{\theta} \equiv \frac{|P_\gamma|}{|v|\sqrt{m_T^2 + m_y^2}} = \frac{mc}{|v|\sqrt{m_T^2 + m_y^2}} = 1 \tag{13}$$

where $m > m_T$, ensuring that v<c and thus preserving causality. The transverse mass of $m_x \equiv m_T$ is missing (effectively frozen in the left-chiral state, as shown in **Figure 2**). Consequently, the total mass (m_{tot}) of the motional system is less than or equal to the missing mass[3].

Where P_r is represented as photon momenta. Majorana fermions annihilate each other, leading to the production of the angle $\bar{\theta} = 0$ (as shown in **Figure 2**) when a photon is radiated. The constraint condition is: $0 \le N \le 1$, a phenomenon not observed in classical physics. The underlying reason is precisely this constraint condition, which is verified in our analysis.

[3]The missing mass depends on experiments.

A detailed discussion of this topic would be extensive and is beyond the scope of this paper. Therefore, it will be presented in a forthcoming publication.

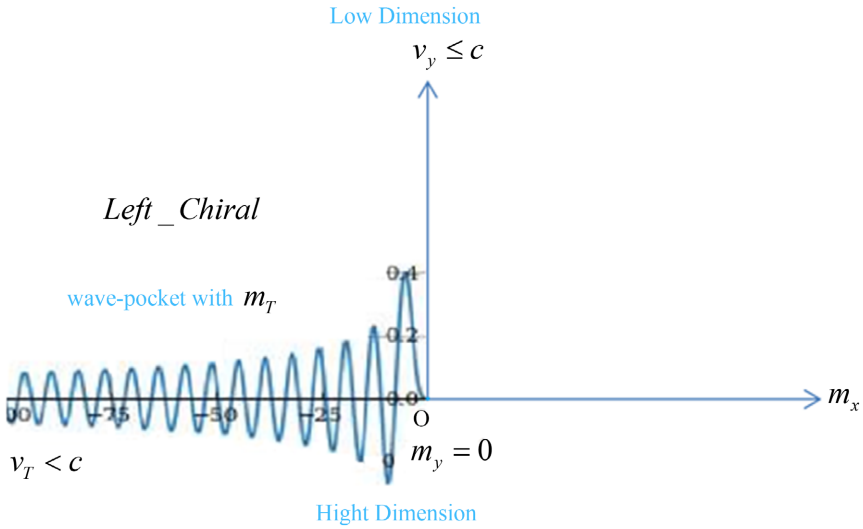

Figure 2. The wave packet of sterile neutrinos is represented using Bessel functions, as shown above. The left-chiral type of sterile neutrinos is missing, leaving only the right-chiral type present, while the nature of the third type remains unknown. The corresponding notation will be provided below.

3.7. Representation: Wave-Pockets of Sterile Neutrinos

Given that $\alpha = 4$ (since $\pi\left(\frac{\pi}{4}\right)^{-1} = 4$), thus produces

$$J_4\left(v_T\right) = \sum_{m=0}^{\infty} \frac{(-1)^m}{4!\Gamma(m+5)}\left(\frac{v_T}{2}\right)^{2m+4}, v_T < c \tag{14}$$

It is easy to see that Eq. (14) generates the wave packet shown in **Figure 2**. Next, by applying the expression for de Broglie matter waves, we obtain:

$$\lambda = \frac{h}{p} = \frac{h}{mv}\bigg|_{v\le c}, m \approx 10^{-14} \sim 10^{-12}\,(\mathrm{eV}) \tag{15}$$

i.e.,

$$0 \sim 10^{-14}\ \mathrm{eV} < m < 10^{-12}\ \mathrm{eV}, c^2 \equiv 1 \tag{16}$$

Evidently, the transverse component is not identified as an axion but rather as a scalar field (e.g., $g_{\alpha\beta}$ possessing extremely small energy[4,5]). This can be determined using gamma-ray bursts, analyzed in terms of the sequence of wavelengths

[4]See Note 7 below as well.

[5]The energy distribution of the wave packet is shown in **Figurre 2** and follows the relationships given in Eqs. (15) - (17), both of which align with the data presented. This agreement arises from the numerical complementarity between the "extremely small magnitudes" described in Eqs. (15) - (16) and the nature of "sterile neutrinos that do not interfere with the current theory of Big Bang nucleosynthesis HNLs" in cosmology.

given below (input conditions of wavelengths):

$$\left.\begin{aligned}\lambda_1 &= \frac{c}{v} = \frac{hc}{10^8\ \text{eV}} = \frac{12400\ \text{eV}\cdot(0.1\ \text{nm})}{10^8\ \text{eV}} = 12400\cdot\left(10^{-18}\right)\text{m} = 1.24\times10^{-14}\ \text{m}\\ &\vdots\\ \lambda_n &= \frac{c}{v} = \frac{hc}{10^5\ \text{eV}} = \frac{12400\ \text{eV}\cdot(0.1\ \text{nm})}{10^5\ \text{eV}} = 12400\cdot\left(10^{-15}\right)\text{m} = 1.24\times10^{-11}\ \text{m}\end{aligned}\right\} \quad (17)$$

where $n>1$ (see Note 7).

In Figure 2, it is important to note that the cross-sectional area of interactions between matter and sterile neutrinos in a vacuum is exactly zero. This result is based on the fact that their longitudinal velocity $|v_y|$ equals the speed of light, *C*.

4. Conclusion

Throughout the history of neutrino research, three types of sterile neutrinos have been theoretically proposed. Based on mechanisms of chiral symmetry breaking, it appears that one of these types—specifically, the left-handed sterile neutrino—was absent in the early universe. The most significant conclusion of this work is that three distinct types of sterile neutrinos may exist: unitary sterile neutrinos corresponding to left- and right-handed states, and a third, as-yet unidentified type. Recent experimental data on neutrino mixing angles further reinforce this framework. In particular, the atmospheric mixing angle is measured to be $\theta_{23} \approx 45^{\circ}{}^{+1.28^{\circ}}_{-1.12^{\circ}}$ suggesting near-maximal mixing, while the solar mixing angle is $\theta_{12} \approx 33.22^{\circ}$ consistent with the standard three-flavor oscillation model. The near-maximal value of θ_{23} may hint at an underlying symmetry or degeneracy among active and sterile states in the early universe. The unexplained absence of the left-handed sterile neutrino introduces a new theoretical puzzle. In this paper, we have discussed this issue in light of current experimental constraints and provided a theoretical commentary based on symmetry breaking and mixing angle observations.

Acknowledgements

We would like to thank Ben Chieu, a graduate of the Department of Physics at CCU, who is currently pursuing studies at the Institute of Computer Science at NTHU.

Author Contribution

The authors contribute equally.

Conflicts of Interest

The authors declare no conflicts of interest regarding the publication of this paper.

References

[1] Zyla, P.A., *et al.* (Particle Data Group) (2020) Review of Particle Physics. *Progress of Theoretical and Experimental Physics*, 083C01.

[2] Yang, C.N. and Mills, R.L. (1954) Conservation of Isotopic Spin and Isotopic Gauge Invariance. *Physical Review*, **96**, 191-195. https://doi.org/10.1103/physrev.96.191

[3] Reich, S. (2012) Neutrino Oscillations Measured with Record Precision. *Nature*, **492**, 190-191.

[4] Barr, S.M. (1984) Solving the Strong CP Problem without the Peccei-Quinn Symmetry. *Physical Review Letters*, **53**, 329-332. https://doi.org/10.1103/physrevlett.53.329

[5] Feng, L., Zhang, J. and Zhang, X. (2017) A Search for Sterile Neutrinos with the Latest Cosmological Observations. *The European Physical Journal C*, **77**, 418. https://doi.org/10.1140/epjc/s10052-017-4986-3

[6] Daya Bay Collaboration (2012) Observation of Electron-Antineutrino Disappearance at Daya Bay. *Physical Review Letters*, **108**, Article 171803.

[7] Boyarsky, A., Drewes, M., Lasserre, T., Mertens, S. and Ruchayskiy, O. (2019) Sterile neutrino Dark Matter. *Progress in Particle and Nuclear Physics*, **104**, 1-45. https://doi.org/10.1016/j.ppnp.2018.07.004

[8] Duff, M.J., Inami, T., Pope, C.N., Sezgin, E. and Stelle, K.S. (1988) Semiclassical Quantization of the Supermembrane. *Nuclear Physics B*, **297**, 515-538. https://doi.org/10.1016/0550-3213(88)90316-1

[9] Majorana, E. (1937) Teoria simmetrica dell'elettrone e del positrone. *Il Nuovo Cimento*, **14**, 171-184. https://doi.org/10.1007/bf02961314

[10] Hooper, D., Silk, J. and Bertone, G. (2008) Particle Dark Matter: Evidence, Candidates, and Constraints. arXiv:hep-ph/0404175v2.

[11] Boyarsky, A., Drewes, M., Lasserre, T., Mertens, S. and Ruchayskiy, O. (2019) Sterile Neutrino Dark Matter. *Progress in Particle and Nuclear Physics*, **104**, 1-45. https://doi.org/10.1016/j.ppnp.2018.07.004

[12] Das, A., Dev, P.S.B. and Okada, N. (2019) Long-lived TeV-Scale Right-Handed Neutrino Production at the LHC in Gauged $U(1)_X$ Model. *Physics Letters B*, **799**, Article 135052. https://doi.org/10.1016/j.physletb.2019.135052

[13] Ibe, M., Kusenko, A. and Yanagida, T.T. (2016) Why Three Generations? *Physics Letters B*, **758**, 365-369. https://doi.org/10.1016/j.physletb.2016.05.025

[14] Particle Data Group, Eidelman, S., *et al.* (2004) Review of Particle Physics. *Physics Letters B*, 592, 1-1109.

[15] Peccei, R.D. (2008) The Strong CP Problem and Axions. In: Kuster, M., Raffelt, G. and Beltrán, B., Eds., *Lecture Notes in Physics*, Springer, 3-17. https://doi.org/10.1007/978-3-540-73518-2_1

[16] Peccei, R.D. and Quinn, H.R. (1977) CP Conservation in the Presence of Pseudoparticles. *Physical Review Letters*, **38**, 1440-1443. https://doi.org/10.1103/physrevlett.38.1440

[17] Nakamura, K. (2010) Review of Particle Physics. *Journal of Physics G: Nuclear and Particle Physics*, **37**, Article 075021. https://doi.org/10.1088/0954-3899/37/7a/075021

[18] Chau, L. and Keung, W. (1984) Comments on the Parametrization of the Kobayashi-Maskawa Matrix. *Physical Review Letters*, **53**, 1802-1805. https://doi.org/10.1103/physrevlett.53.1802

[19] Cabibbo, N. (1963) Unitary Symmetry and Leptonic Decays. *Physical Review Letters*, **10**, 531-533. https://doi.org/10.1103/physrevlett.10.531

[20] Kobayashi, M. and Maskawa, T. (1973) *CP*-Violation in the Renormalizable Theory of Weak Interaction. *Progress of Theoretical Physics*, **49**, 652-657.

https://doi.org/10.1143/ptp.49.652

[21] Hu, B.Z. (On Behalf of the Daya Bay Collaboration) (2015) Recent Results from the Daya Bay Reactor Neutrino Experiment. arXiv:1505.03641v1.

[22] An, F.P., Bai, J.Z., Balantekin, A.B., Band, H.R., Beavis, D., Beriguete, W., *et al.* (2012) Observation of Electron-Antineutrino Disappearance at Daya Bay. *Physical Review Letters*, **108**, Article 171803.

[23] Beauregard, R.A. and Fraleigh, J.B. (1973) A First Course in Linear Algebra: With Optional Introduction to Groups, Rings, and Fields. Houghton Mifflin Co.

[24] Bronson, R. (1970) Matrix Methods: An Introduction. Academic Press.

[25] Horn, R.A. and Johnson, C.R. (1985) Matrix Analysis. Cambridge University Press.

Appendices

Appendix A: Some Useful Calculations or Expressions in Detailed Process

Table S1. The calculation in previous progression.

In progress:

Starting with

$$J_\alpha(v_T)=\sum_{m=0}^{\infty}\frac{(-1)^m}{m!\Gamma(m+\alpha+1)}\left(\frac{v_T}{2}\right)^{2m+\alpha},v_T<c \tag{A.1}$$

For $\alpha=4$,

Detailed deductions:

I) In Mie scattering, when $\alpha^2\equiv n(n+1)$ (i.e., scattering centers approach a state of rest), electromagnetic waves in the form of *sinc* functions appear in the screen regions.

II) For $0<v_T\ll\sqrt{\alpha+1}$, Bessel functions correspond to higher-dimensional representations, indicating that matter waves exhibit asymptotic behavior.

III) The above deductions suggest that photons and sterile neutrinos can interconvert with certain probabilities—this represents a new breakthrough.

$$J_4(v_T)=\sum_{m=0}^{\infty}\frac{(-1)^m}{4!\Gamma(m+5)}\left(\frac{v_T}{2}\right)^{2m+4},v_T<c \tag{A.1}$$

Results—The shape of the wave packet is determined as follows:

The shape of the wave packet is determined as follows:

A wave packet must be expanded using Eq. (A.1), where $x\equiv v_T<c$ Here, m represents the order of the Bessel functions, which characterize the structure and behavior of the wave packet.

Appendix B: Obtaining $\alpha=4$

In Table S1, the consecutive use of $\alpha=4$ is justified by Bessel's integrals. This follows the Hansen-Bessel formula for integer values of $\alpha=4$, based on observations of its cosine components:

$$J_\alpha(z)=\frac{1}{\pi}\int_0^{\pi}\cos(x\sin\theta-\alpha\theta)\mathrm{d}\theta,\theta\equiv\delta_{CP} \tag{A.3}$$

Evidently, through observation, it is defined as $\alpha\theta\equiv\pi$. Since the previous discussion denoted θ as $\theta=\frac{\pi}{4}$, it follows that $\alpha=4$ exactly.

Appendix C: Finding the Transform Probability of the Third Type Sterile Neutrinos

Here, using a physical-mathematical approach, we determine the probability of the transformation of the third type of sterile neutrinos into photons or gravitons. To proceed, we consider three essential functions from advanced physical mathematics:

$$\lim_{A_1\to 0}\frac{1}{A_1}\sin c\left(\frac{u}{A_1}\right)\Big|_{u=v=c}=\delta(c) \tag{A.4}$$

$$\int_0^\infty xJ_\alpha(ux)J_\alpha(vx)\mathrm{d}x\Big|_{u=v=c}=\frac{1}{u}\delta(u-v)\Big|_{u=v=c}=\frac{1}{c} \tag{A.5}$$

$$\int_{-\infty}^{\infty}\delta(u-v)\mathrm{d}u\Big|_{u=v=c}=\delta(0)=1 \tag{A.6}$$

All of these equations correspond to Figure 2 based on observation. Eq. (A.4) represents the shape of the wave packet, where A_1 corresponds to photons. Eq. (A.5) is the closure equation of Bessel functions, associated with the delta function. Eq. (A.6) describes the impulse of the wave packet curve for the third type of sterile neutrinos traveling through the universe and their transformation into photons or gravitons.

All these equations hold at the speed of light C (along the y-axis in Figure 2). When derived at the point $v=c$, they yielded the same zero slope (i.e., a horizontal line), indicating a stable propagation condition. Note that the wave packets of the third type of sterile neutrino, corresponding to Bessel functions $(v=c)$, are described by Eq. (A.5). This reveals the possibility of their transformation into photons or gravitons. The probability of this transformation can be calculated using the delta function in Eq. (A.6) within the framework of quantum mechanics, as shown below. The detailed transformation of photons can be found in Table S2.

Appendix D: Transform Probabilities in Qm

Here, we directly derive the following calculations based on observation:

Using Eqs. (A.4) and (A.6), and considering all types of sterile neutrinos traveling through space with the passage of time (i.e., applying the Fourier transform), we obtain:

$$\int_{-\infty}^{\infty}\sin c(t)\mathrm{e}^{-i2\pi ft}\mathrm{d}t=rect(f)=\begin{cases}0, |f|>\frac{1}{2}\\ \frac{1}{2}, |f|=\frac{1}{2}\\ 1, |f|<\frac{1}{2}\end{cases} \tag{A.7}$$

This analysis reveals the probability of distribution for sterile neutrinos transforming into other particles. As discussed in **Appendix C**, the probability of the third type of sterile neutrinos transforming into photons or gravitons is 1/2 (i.e., 50%) (see Figure S1).

For the other types: A probability of zero applies to both the first type (missing left-chiral) and the second type (right-chiral) sterile neutrinos, indicating that their transformation into photons or gravitons is forbidden. The term $rect(f)=1=100\%$ represents the top-point of A_1, corresponding to photons transforming into themselves (i.e., no transformation, but an intrinsic probability

of 1, as dictated by their spin[6]). Additionally, Eq. (A.7) aligns with the triangular nature observed in mathematical physics, as depicted in Figure S3. The Feynman diagram (F.D.), confirming that quanta in scalar fields are forbidden from utilizing this property. The running points along the two isosceles sides may correspond to gauge fermions (i.e., the first and second types of sterile neutrinos), which also conform to Feynman diagrams (F.D.). The second and third types of probabilities in Eq. (A.7) correspond to particle spins of 1/2 (fermions) and 1 (photons), respectively. As gauge fermions move along the running points at A_1, they naturally transform into photons with a probability of 50% or less such as 3/8 (the concept of critical density, see "Friedmann equations")—a key feature of this framework (see Figure S3 for detailed visual interpretations.) By consideration of the KK-Theory, if analyzed within the Kaluza-Klein (KK) theory, the transformation of A_1 (photons/gravitons) is permitted when quanta are coupled to each other. This suggests a deeper connection between higher-dimensional gauge theories and sterile neutrino interactions.

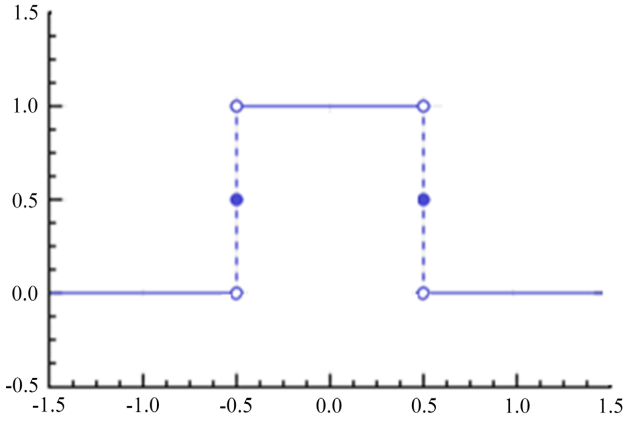

Figure S1. The rectangle functions.

Appendix E: Origins of Neutrino Masses

In physics history, neutrinos oscillation problem attracts experimental study and theoretically researches in particle physics widely. In 1998, Kajita Takaaki found the phenomena of neutrinos oscillation and then with Arthur McDonald commonly verified neutrinos possessing their masses. According to quantum mechanics, if the quantum number of flavor of particles is changed, they must have masses, it is interesting. However, they did not explain why neutrinos possess their corresponding three mass values respectively in terms of the underlying mechanism or the exact mass spectrum.

[6]1) It is truly remarkable that this fact has been discovered. Its uniqueness lies in the intrinsic properties of gauge bosons—specifically, the delocalization in quantum mechanics (QM), which leads to the exclusion of the first formula in Eq. (A.7). This exclusion implies a constraint: quanta in scalar fields cannot utilize this property at the top-point of A_1 (a fundamental characteristic in mathematical physics).

2) See section: Key-Observations.

The Mass Spectrum: In the history of physics, the neutrino oscillation problem has attracted extensive experimental and theoretical research in particle physics. In 1998, Kajita Takaaki discovered the phenomenon of neutrino oscillation, and together with Arthur McDonald, they confirmed that neutrinos possess mass. According to quantum mechanics, if a particle's flavor quantum number changes, it must have mass—an intriguing property. However, their work did not explain why neutrinos have three distinct mass values, specifically in terms of

$$m_{\upsilon_e} < 2.2 \text{ eV}, m_{\upsilon_\mu} < 1.7 \text{ MeV}, m_{\upsilon_\tau} < 15.5 \text{ MeV}, c^2 \equiv 1 \tag{A.8}$$

In the current Standard Model (SM), this remains an unresolved mystery.

In this paper, we introduce an "isosceles trapezoid" method and a matrix transformation model to address this issue comprehensively. Specifically, we propose that V_3' in the CKM matrix is absorbed by $g_{a\beta}$ based on $i\delta = i/2$ (a process we refer to as "CKM absorption"), providing a well-structured solution to this problem.

Key-Observations:

The top-point of A_1 (photons) aligns with Feynman diagram's scattering top-point. In this paper we propose that neutrino masses acquire their values through a mechanism based on the "isosceles trapezoid" model. This model represents a tangent plane, which is a part of the world-volume of an electron, as discussed in previous sections. The electron mass transfers a portion of its eigen-mass to neutrinos, and ongoing calculations further explore this process. As shown in **Figure S2**, we analyze the difference in the Lorentz factor between $v \approx 0.06325c, \gamma \approx 1.002$ and $v = 0, \gamma = 1$. Therefore,

$$\Delta\gamma = 1.002 - 1 = 0.002 \tag{A.9}$$

Calculation for A, thus we obtain

$$A = \frac{1}{10^5 - 0.002}, \text{ for all neutrinos} \tag{A.10}$$

$\gamma = 10^5$ occurs at $t = 10^{-6}$ s. In sequence,

$$A_1 = 0 \tag{A.11}$$

(i.e., the top point of the height corresponds to massless photons ($\gamma = \infty$))

As the flavor changing of $\tan\theta|_{\theta=0} = 0$ occurs, it corresponds to the height of the isosceles trapezoid. The flavor change takes place precisely at this height, which is identified as the point where photons emerge. And[7]

[7]In the ensemble of electrons and υ_e, the "electric field correction" requires that $\gamma = 29.30$ due to the non-effected dipole presentation of particles, similar to the well-known muon g−2 precession problem. It has been confirmed that neutrinos do not possess electric dipoles, which explains why they do not participate in electromagnetic interactions. $\gamma = 29.30$ represents the turning point where the electron's world-volume transforms into neutrinos as they acquire mass. This process naturally aligns with momentum conservation law. However, not the speed of neutrinos, but rather $\gamma = 10^5$, which governs their transformation—an unexpected yet fundamental result.

$$2\gamma = 2\cdot \underbrace{(29.30)}_{\text{magic.momentum}} = B_1 \quad \text{for} \quad \nu_\tau \tag{A.12}$$

with the corresponding angle of $\theta = 63.43^\circ$ and a factor of $\tan(63.43^\circ) = 2$ produced. In sequence,

$$0.2\gamma = (0.2)(29.30) = B_2 \quad \text{for} \quad \nu_\mu \tag{A.13}$$

with the corresponding angle of $\theta = 11.31^\circ$ and a factor of $\tan(11.31^\circ) = 0.2$ produced, eventually, $\gamma_e \cdot (0.511\,\text{MeV})$ is defined as the height. Here, A and B represent motional lengths, which can be adjusted accordingly. By applying the formula for the area, we obtain the followings: ν_e mass given by

$$m_{\upsilon_e} = \begin{cases} \frac{1}{2}\frac{A_1 h}{2} = 0 \\ \frac{1}{2}\frac{Ah}{2} = \frac{0.511\,\text{MeV}}{4}\frac{1}{10^5 - 0.002} \approx 1.2775\,\text{eV} < 2.2\,\text{eV} \end{cases} \tag{A.14}$$

where the factor of $\frac{1}{2}$ arises due to CP violation[9], which corresponds to taking half the area of the isosceles triangle shown in **Figure S3**. Following the same approach, we construct the mass formulation as follows: ν_τ mass given by

$$m_{\upsilon_\tau} = \frac{(A+B)h}{2} = \frac{\left(\frac{1}{10^5 - 0.002} + (2)(29.30)\right)(0.511\,\text{MeV})}{2} \approx 14.9723\,\text{MeV} < 15.5\,\text{MeV} \tag{A.15}$$

ν_μ mass given by

$$m_{\nu_\mu} = \frac{(A+B)h}{2} = \frac{\left(\frac{1}{10^5 - 0.002} + (0.2)(29.30)\right)(0.511\,\text{MeV})}{2} \approx 1.4972\,\text{MeV} < 1.7\,\text{MeV} \tag{A.16}$$

where $c^2 \equiv 1$. All of the results align with current experimental data and comply with the Standard Model. We define the area of the isosceles trapezoid as the "battle array" of flavor changing with time variation, representing the dynamic nature of neutrino oscillations and mass generation.

Here, $A_n = \{A_1, A_2, A_3, \cdots\}$, $B_n = \{B_1, B_2, B_3, \cdots\}$, and H varies with the electron's Lorentz factor γ. Additionally, $A_1 = 0$ represents a massless photon, revealing that photons play a role in the mechanism through which neutrinos acquire their masses. We will discuss this further in later sections. This method also clearly explains why neutrinos do not participate in electromagnetic interactions. Its validity can be confirmed through the angle of $\pi/4$, which is represented as follows.

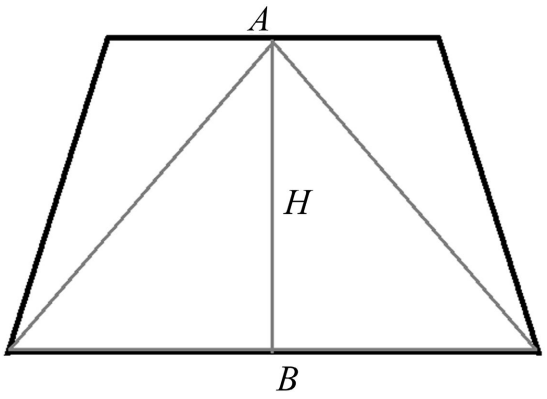

Figure S2. The seesaw: $\frac{(A+B)H}{2}$ represents neutrino masses. This approach provides an effective and elegant resolution to the long-standing problem of neutrino masses within the framework of modern particle physics. The resulting mass hierarchy emerges naturally and corresponds to what is widely known as the "seesaw" mechanism, which may be interpreted as a complete and self-consistent theoretical framework.

Appendix F: Rules of CKM Absorption

Due to the CKM matrix, through the mixing angles associated with $\theta = 63.43^\circ$ and $\theta = 11.31^\circ$, we obtain

$$\theta_{mix} \equiv \bar{\theta} = \frac{63.43^\circ \pm 11.31^\circ}{2} = \begin{cases} 37.37^\circ \\ 26.06^\circ \end{cases} = \frac{N(N-1)}{2} \tag{A.17}$$

Yields

$$N(N-1) = 2\bar{\theta} \tag{A.18}$$

In this paper, we have utilized the matrix 2×2, ensuring that $N = 2$ to account for two mixing angles as described above, along with one CP-violation phase.

For the 2×2 matrix, its form appears as:

$$\delta_{CP} \equiv \left.\frac{N-1}{2}\right|_{N=2} = \frac{1}{2} \tag{A.19}$$

Or, in the case of $N = 2$ (known as the "Cabibbo angle 13.03°", introduced by Dr. Nicola Cabibbo), the matrix can be expressed in terms of complex numbers.

Due to the presence of independent variables, only one term of …\dots… remains separated from $\frac{N-1}{2}$, leading to the following form:

$$\frac{(N-1)(N-2)}{2} \tag{A.20}$$

And this factor is permitted to be used only once, specifically for the first generation ν_e. Notably, based on Supersymmetry (SUSY) and chaos theory, the quarks in the CKM matrix can be fully applied to neutrinos in this framework. Additionally, these findings can be compared with the results of

$$\theta_{12} \equiv \frac{\theta_{mix_1} + \theta_{mix_2}}{2} = \frac{37.37^\circ + 26.06^\circ}{2} = 37.715^\circ \tag{A.21}$$

This reveals the difference between ±4.495˚ and the experimental result of $\theta_{12} \equiv \theta_{sol} \approx 33.22^{\circ}$. The percentage error is approximately 13.531% < 13.80%, which falls within the acceptable range of astrophysical errors and remains valid when analyzed using the least squares method.

As far as we know, how do neutrinos acquire their masses? Due to $A_1 = 0$, the overall symmetry of flavor quantum numbers is preserved, leading to its absence in the Standard Model (SM). While flavors remain unchanged, their underlying nature constructs the mechanism by which neutrinos acquire mass.

The key-answer is that the metric tensor of $g^{\alpha\beta}$ is absorbed by the CKM matrix within the electromagnetic stress-energy tensor, thereby incorporating $g^{\alpha\beta}$ as elements of the CKM matrix. As a result, neutrinos acquire their masses.
It is widely known that

$$T^{\alpha\beta} = \frac{1}{4\pi}\left(-F^{\alpha\gamma}F_{\gamma}^{\beta} - \frac{1}{4}g^{\alpha\beta}F_{\gamma\delta}F^{\gamma\delta}\right) \tag{A.22}$$

The absorption is clearly located in the second term of Eq. (A.22).

Binos were exchanged with sgluons at $t < 10^{-6}$ s, and subsequently, sgluons transformed into gluons at $t \geq 10^{-6}$ s due to SUSY breaking. Electrons, as commonly understood, are composed of gluons and quarks. By losing a small portion of their world-volume, electrons could transfer mass to neutrinos, allowing neutrinos to acquire their eigenstates of mass. The electromagnetic stress–energy tensor interacts with the hyperplane through this mechanism. This is facilitated by the constant flux of $x^{\beta} = const$, ensuring the probability of neutrinos being marked on this plane of

$$\sum_{i=1}^{\infty} a_i x_i = b \tag{A.23}$$

Evidently, the sectional area of x^{β} represents the interaction between neutrinos and gravity. This interaction passes through the momentum components of α in $T^{\alpha\beta}$—which corresponds to the electromagnetic (EM) stress-energy tensor, the photon's contribution to the gravitational source. As a result, neutrinos acquire their masses from the scalar field of ϕ which can arise from three possible mechanisms: Gravitational potentials (in the case of the current universe, where this process could be attributed to photon mass-energy). Inflationary repulsive potentials (in the early universe at $t = 10^{-6}$ s). Scalar fields based on Supersymmetry (SUSY).

Presented as a model where neutrinos acquire mass by absorbing the metric tensor $g_{\alpha\beta}$. We have found that the Cabibbo-Kobayashi-Maskawa (CKM) matrix[8] shares the same mathematical structure as the metric tensor $g_{\alpha\beta}$. Considering a

[8]Particular, exchanges of $U_{CKM} \approx U_{MNS}, m_{quarks} = m_{neutrinos} = 0$, and $\delta_{CP} \equiv \delta_{13} \pm 2\varphi, \varphi \leq 45^{\circ}$. The chaotic behavior is permitted under high-energy conditions, particularly in the context of $m_{quarks} = m_{neutrinos} = 0$. Here, $U_{CKM} \approx U_{MNS}$ and $\delta_{CP} \equiv \delta_{13} \pm 2\varphi, \varphi \leq 45^{\circ}$ can be linked to **Eq. (A.38)**, which will be discussed in later sections (see **Ref. [19]**).

local coordinate system of x^i, the metric tensor is denoted as $g_{\alpha\beta}$ or *G*. Therefore,

$$G = \left(g_{\alpha\beta}\right) = J^{\mathrm{T}} J = \begin{bmatrix} 1 & 0 \\ 0 & r^2 \end{bmatrix} \tag{A.24}$$

It is readily observed that these calculated matrix results align with those in the CKM matrix (derived due to $V_2' V_1' V_3'$), as demonstrated in Refs. [16], [18].

$$V_3' = \begin{bmatrix} 1 & 0 & 0 \\ 0 & c_3 & s_3 \\ 0 & -s_3 & c_3 \end{bmatrix} \tag{A.25}$$

And,

$$V_3' = \begin{bmatrix} 1 & 0 & 0 \\ 0 & c_3 & s_3 \\ 0 & -s_3 & c_3 \end{bmatrix} = 1 \tag{A.26}$$

If we exclude complex numbers (i.e., due to Eq. (A.19), the complex phase of $i\delta = \frac{i}{2}$ is explicitly broken, leading to CP violation. Consequently, V_3' becomes a real $\left(v_{11}\right)$ matrix of G where the element V_3' corresponds to the covariant component of $g_{\alpha\beta}$, which can be absorbed into the matrix. From Eq. (A.23), we have derived:

$$x^{\beta} = const \tag{A.27}$$

This implies that neutrino coordinate systems are defined on the hyperplane. Following the mechanism outlined earlier (see the section "Momentum-components of α in $T^{\alpha\beta}$"), neutrinos acquire mass by "absorbing" $g_{\alpha\beta}$ contributions mediated by photons. This "CKM-like absorption" is fundamentally a coupling process, making the absorption direction irrelevant. The small magnitude of neutrino masses can be understood through Eqs. (A.14) - (A.16) and Figure S2).

Remark.

Here

$$c_3 \equiv \cos\theta_3, \text{ and } s_3 \equiv \sin\theta_3 \tag{A.28}$$

We have fully resolved the origin of neutrino masses. Specifically, we propose that neutrinos acquire mass by absorbing photon mass-energy (see Eq. (A.22)) over cosmological timescales—from the early universe (e.g., the post-inflation at $t = 10^{-6}$ s) to the present epoch. This process contributes to dark matter phenomenology (with neutrino critical density ρ_v playing a key-role). The mechanism $\alpha_1 = \alpha_2 = 0$ has been rigorously validated via cross-validation (e.g., competitive mechanisms) for neutrinos as Majorana fermions. According to basic definitions of

$$\cos(i\delta) = \cosh\delta \equiv \frac{e^{\delta} + e^{-\delta}}{2} \tag{A.29}$$

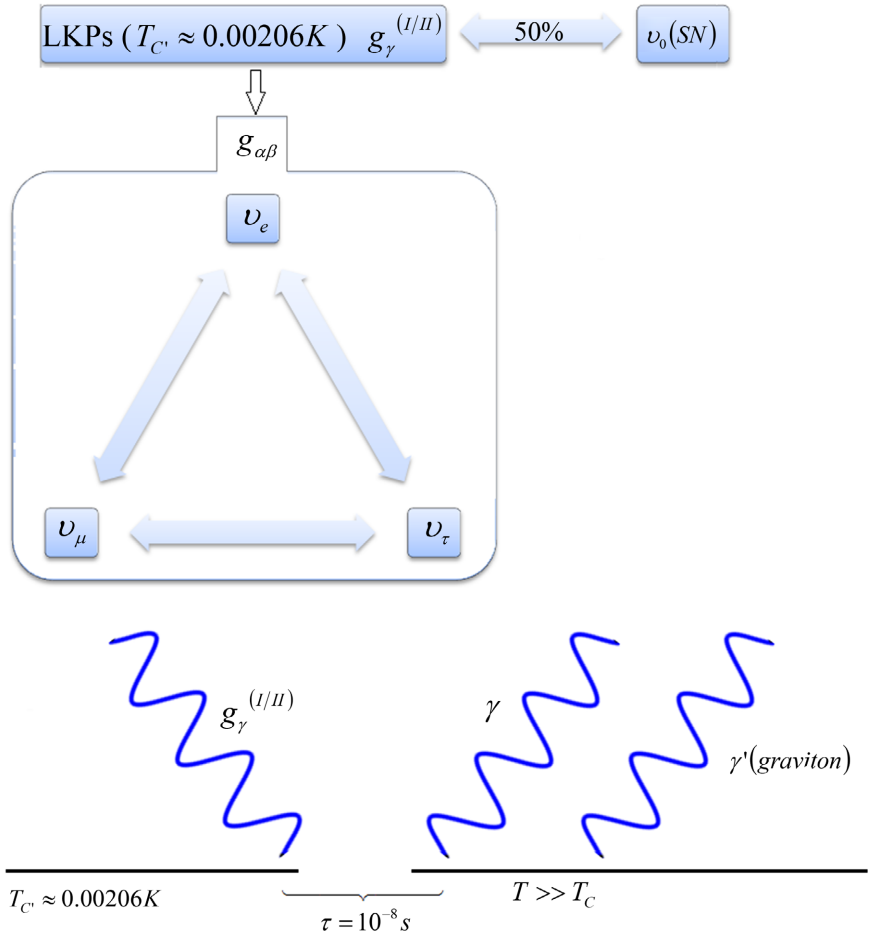

Figure S3. The relationships for massless particles in this paper, where υ_0 is denoted as sterile neutrinos, and $g_{\alpha\beta}$ leads the bucket as a sea of $g_{\alpha\beta}$, are discussed. The widely-known Casimir temperature $T_C \approx 0.00206\,\mathrm{K}$ was calculated by the first author in a private manuscript.

And,

$$\sin(i\delta) = \sinh\delta \equiv \frac{e^{\delta} - e^{-\delta}}{2} \tag{A.30}$$

This hyperbolic geometry is illustrated in **Figure S4**. Given its structural similarity to **Figure S2**, we position $A_1 = 0$ photons at point O and neutrinos B_n at their respective side-lengths. Mathematically, we consider half of the area bounded by these two hyperbolic functions. Notably,

$$\cos(i\delta)\big|_{\delta=1/2} = \cosh\left(\frac{1}{2}\right) \equiv \frac{e^{\frac{1}{2}} + e^{-\frac{1}{2}}}{2} \approx 1.1276 \quad \text{in radian} \tag{A.31}$$

And,

$$\frac{\sin(i\delta)\big|_{\delta=1/2}}{2}=\frac{\sinh\left(\frac{1}{2}\right)}{2}\equiv\frac{e^{\frac{1}{2}}-e^{-\frac{1}{2}}}{4}\approx 0.2606 \quad \text{in radian} \tag{A.32}$$

where for $\sinh x, \forall x \geq 1$, it must be added $x=1$ in this case, due to the mathematical nature of moving in *x-axis* shown as **Figure S4**:

$$1+\frac{\sinh(\delta)\big|_{\delta=1/2}}{2}\approx 1.2606 \quad \text{in radian} \tag{A.33}$$

Comparing with the obtained data of [16]

$$\delta_{13}=1.2\pm 0.08 \tag{A.34}$$

Remark.

$(1.1276)\times 180^{\circ}=202.968^{\circ}$. This alignment matches the behavior δ_{13} in the CKM matrix and parallels the δ_{CP} in PMNS matrix under chaotic conditions. These matrices act as similarity transformations governing the relationships of $\delta_{CP}=\delta_{13}\pm 45^{\circ}$ in earlier expressions (e.g. [19]). For instance:

$$\begin{aligned} 246^{\circ} &\cong 202.968^{\circ}+45^{\circ} \\ 169^{\circ} &\sim 202.968^{\circ}-45^{\circ} \end{aligned} \tag{A.35}$$

in radian by experiment observations (obtained by least squares), we find that Eq. (A.34) matches (1.2 − 0.08) and Eq. (A.36) matches (1.2 + 0.08) in radians, respectively. Thus, the reversal solution corresponds to the reference angle of the CP-violation phase $\frac{\delta}{2}=\frac{1}{4}$ (expressed in non-radian units)—as results.

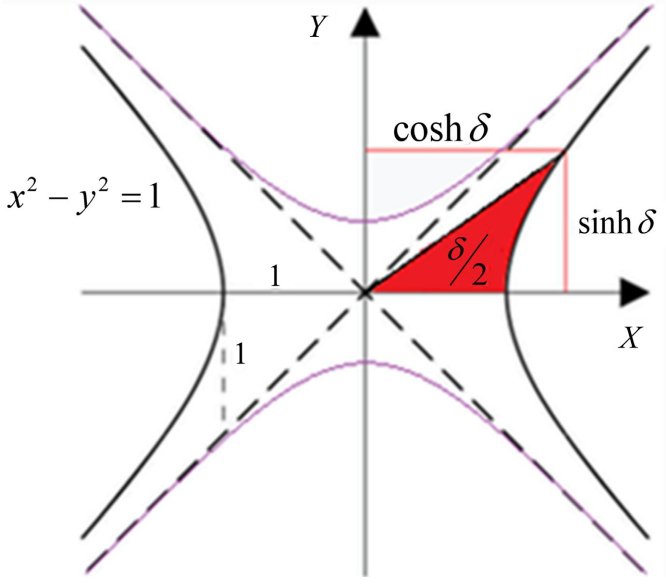

Figure S4. The phase angle of CP violation in neutrinos is determined using hyperbolic functions. Notably, the lower half-sections enclosed by $\sinh\delta$ and $\cosh\delta$ resemble the shape of the isolated trapezoid depicted in **Figure S2.** Strongly supported by Ref. [17].

Furthermore, when expressed in radians and analyzed on the *xy*-plane, this corresponds to $\left|\pm\frac{\pi}{4}\right| \equiv |\varphi| = |\pm 45^\circ| \le 45^\circ$ as the starting point of the CP-violation phase angle "basement", where $A_1 = 0$ (photons) are excluded. Here, A_1 serves as the gauge symmetry reference point for neutrinos. This resolves the long-standing mystery of neutrino mass origins. The above analysis demonstrates that our proposed isosceles trapezoid framework is mathematically consistent.

Remark.

$(0.2606)\times 180^\circ = 46.908^\circ$ where it is good according with $\theta_{23} = 47.9^\circ$ in U_{PMNS}, note that this analysis needs to be disputed.

Remark.

$(1.2606)\times 180^\circ = 226.908^\circ$ Such accords with phase angle of δ_{13} in UCKM, e.g.

$$\left.\begin{aligned}(1.20+0.08)\times 180^\circ = 230.4^\circ \cong 226.908^\circ\\ (1.20-0.08)\times 180^\circ = 201.6^\circ \sim 226.908^\circ\end{aligned}\right\} \quad \text{(A.36)}$$

Nouvelle mysteries: Particularly, here we have "similarities" [23]-[25] as below that it is quite mysterious,

$$|\Delta\theta|_A \equiv 230.4^\circ - 226.908^\circ = 3.492^\circ \sim 2.44^\circ \left(U_{CKM}\right) \quad \text{(A.37)}$$

And

$$|\Delta\theta|_B \equiv 226.908^\circ - 201.6^\circ = 25.308^\circ \cong 194^\circ - \delta_{CP} = 25^\circ \left(U_{PMNS}\right) \quad \text{(A.38)}$$

This leaves unknown reasons that need to be further examined through study or research, especially in emergency situations.

Appendix G: Profiles of Photons

Table S2. An important show for amazing photons. The table provides a structured and logical summary of the synthesized findings based on the overall argumentation presented in this study.

Masses	$m_0 = 0$	Massless particles with representation of p^2 (see previous sections).
Flavor quantum numbers	0	No flavors.
Symmetry	Total symmetrical center of flavors	$\bar{\theta} = 0$, and could be produced by $\beta\beta$-decays without neutrinos in an experiment considered by this paper.
Super-partners in this paper	The third type of sterile neutrinos (i.e., A_1-SN) with probabilities of transform of 1/2.[a]	While SUSY is broken. Recommend it as the same as indicated as *neutralinos* $\left(\tilde{\chi}_1^0, \tilde{\chi}_2^0, \tilde{\chi}_3^0, \tilde{\chi}_4^0\right)$. Where $\tilde{\chi}_1^0$ were used by NLSPs of gravitinos. See **Figure S5**.
SUSY	Stands completely.	Located on the point of A_1.

[a]In this case, $h\nu = 10^8$ eV, could see the denominator in first formula by Eq. (17).

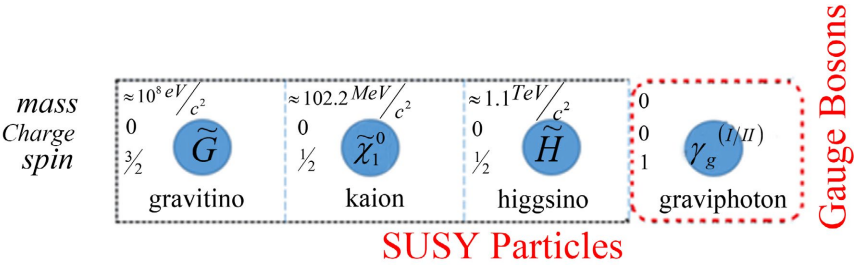

Figure S5. The sequence for populating a gravitino and a $\tilde{\chi}_1^0$ supersymmetric particle (NLSP) within hypothetical SUSY particle frameworks remains debatable. Notably, the graviphoton (LKP I/II) exhibits a motional mass of $h\nu = 10^8\ \mathrm{eV/c^2}$ (as calculated by the first author) and a vanishing rest mass $\left(m_{rest} = 0\right)$, respectively. The gravitino and $\tilde{\chi}_1^0$ masses and their spins, respectively, calculated by the first author.

Remark.

In 1980s, the existence of the Higgs field had not yet been confirmed, and at that time, quark field theory was popular. Therefore, $\delta_{13} \approx \dfrac{2.273^\circ}{2}$, a half of 2.273° scientifically accepted reliable estimated data can be considered acceptable. The key point is that the value of this angle depends on the type of physical field theory being discussed, rather than being a fixed, unchanging result.